THE JOURNAL OF BIOLOGICAL CHEMISTRY VOL. 284, NO. 50, pp. 34723–34734, December 11, 2009

Forkhead-associated Domain-containing Protein Rv0019c and Polyketide-associated Protein PapA5, from Substrates of Serine/Threonine Protein Kinase PknB to Interacting Proteins of *Mycobacterium tuberculosis*[*] [S]

Received for publication, August 25, 2009, and in revised form, October 9, 2009 Published, JBC Papers in Press, October 13, 2009, DOI 10.1074/jbc.M109.058834

Meetu Gupta[‡§1], **Andaleeb Sajid**[‡2], **Gunjan Arora**[‡1], **Vibha Tandon**[§¶], **and Yogendra Singh**[‡3]

From the [‡]*Institute of Genomics and Integrative Biology, Council of Scientific and Industrial Research, Delhi 110007, and the* [§]*Dr. B. R. Ambedkar Center for Biomedical Research and the* [¶]*Department of Chemistry, University of Delhi, Delhi 110007, India*

Mycobacterium tuberculosis **profoundly exploits protein phosphorylation events carried out by serine/threonine protein kinases (STPKs) for its survival and pathogenicity. Forkhead-associated domains (FHA), the phosphorylation-responsive modules, have emerged as prominent players in STPK mediated signaling. In this study, we demonstrate the association of the previously uncharacterized FHA domain-containing protein Rv0019c with cognate STPK PknB. The consequent phosphorylation of Rv0019c is shown to be dependent on the conserved residues in the Rv0019c FHA domain and activation loop of PknB. Furthermore, by creating deletion mutants we identify Thr^{36} as the primary phosphorylation site in Rv0019c. During purification of Rv0019c from *Escherichia coli*, the *E. coli* protein chloramphenicol acetyltransferase (CAT) specifically and reproducibly copurifies with Rv0019c in a FHA domain-dependent manner. On the basis of structural similarity of *E. coli* CAT with *M. tuberculosis* PapA5, a protein involved in phthiocerol dimycocerosate biosynthesis, PapA5 is identified as an interaction partner of Rv0019c. The interaction studies on PapA5, purified as an unphosphorylated protein from *E. coli*, with Rv0019c deletion mutants reveal that the residues N-terminal to the functional FHA domain of Rv0019c are critical for formation of the Rv0019c-PapA5 complex and thus constitute a previously unidentified phosphoindependent binding motif. Finally, PapA5 is shown to be phosphorylated on threonine residue(s) by PknB, whereas serine/threonine phosphatase Mstp completely reverses the phosphorylation. Thus, our data provides initial clues for a possible regulation of PapA5 and hence the phthiocerol dimycocerosate biosynthesis by PknB, either by direct phosphorylation of PapA5 or indirectly through Rv0019c.**

Genes encoding serine/threonine protein kinases (STPKs)[4] once thought to be unique to eukaryotes are now an established integral component of many prokaryotic genomes (1–5). The coordinated action of STPKs with a cohort of protein modules leads to the formation of numerous signaling cascades essential for cell survival. Various protein modules that recognize phosphopeptide binding sites typically exposed after kinase autophosphorylation have been the subject of active research in the past few years (6). In eukaryotes such an association is best exemplified by the binding of proteins containing Src homology 2 domains with phosphotyrosyl residues of activated receptor tyrosine kinases (7). In parallel with tyrosine kinase signaling, the eukaryotic serine/threonine protein kinases associate with various phosphopeptide binding modules, namely, 14-3-3, WW, Polo-box, and FHA domains (6). Of these FHA domains, the phosphothreonine binding modules are uniquely found in prokaryotes to higher eukaryotes (8).

FHA domains were first identified as a conserved region of ~75 amino acids through sequence analysis in a subset of forkhead-type transcription factors (9). Subsequent biochemical and structural studies revealed that the functional FHA domain spans ~100–150 amino acids and flanks beyond the FHA core homology region were required to form a stable 11-stranded β sandwich structure (10–12). FHA domains share very low sequence homology, with only seven conserved residues in more than 65% of known FHA domains (13). The conserved residues are interspersed in loops connecting β strands and are clustered in close proximity to form an interaction with the phosphothreonine residue and the peptide backbone of the interacting protein (14). Initially identified in 20 proteins from yeast, mammals, and bacteria (9), FHA domains are now known to be a part of 2554 unrelated proteins from bacteria to humans. In eukaryotes, FHA domain-containing proteins play crucial roles in diverse cellular processes such as cell cycle regulation, DNA damage response, protein degradation, vesicular transport, and signal transduction (15).

Although a wealth of information is available on the function of FHA domains in eukaryotes, their role in prokaryotic biology is only beginning to unravel (16). The information acquired in the past few years point toward their roles in secretion pathways, transcription, cellular metabolism, and signal transduction (17–21). Among prokaryotes, *Mycobacterium tuberculosis* has emerged as an attractive model system for understanding

* This work was supported by Council of Scientific and Industrial Research Grant NWP-0038.

[S] The on-line version of this article (available at http://www.jbc.org) contains supplemental Fig. S1.

[1] Senior Research Fellows of the Council of Scientific and Industrial Research, India.

[2] Senior Research Fellow of the University Grants Commission, India.

[3] To whom correspondence should be addressed: Mall Road, Delhi 110007, India. Tel.: 11-2766-6156; Fax: 11-2766-7471; E-mail: ysingh@igib.res.in.

[4] The abbreviations used are: STPK, serine/threonine protein kinase; FHA, forkhead associated; GST, glutathione *S*-transferase; CAT, chloramphenicol acetyltransferase; ELISA, enzyme-linked immunosorbent assay; PIPES, 1,4-piperazinediethanesulfonic acid.

FHA domain-mediated signaling for two reasons: 1) *M. tuberculosis* encodes for 11 eukaryotic like STPKs (PknA to PknL, except PknC) and seven FHA domains in six proteins (22), thus offering an experimentally malleable system to understand molecular themes common to prokaryotes and eukaryotes. 2) Recent studies show that STPKs play an important role in *M. tuberculosis* survival and pathogenicity (23) and FHA domains are known to play a key role in STPK-mediated signaling events.

Biochemical studies carried out on three FHA domain-containing proteins of *M. tuberculosis* have provided unambiguous evidence for their involvement in STPK-mediated signal transduction pathways crucial for *M. tuberculosis* virulence. EmbR, a SARP family transcription factor, was shown to act downstream of PknH in a FHA domain-dependent manner to upregulate embCAB arabinosyltransferases, resulting in a higher LAM/LM ratio, an important determinant of mycobacterial virulence (24–26). Rv1747 (ABC transporter), a component of PknF-mediated signal transduction and the only protein comprised of two FHA domains, was shown to be important for *M. tuberculosis* growth in macrophages and mice (27). Recent work on GarA, a small protein mainly occupied by the FHA domain, has provided an indirect link to the regulation of the mycobacterial metabolism by STPKs PknB and PknG (28, 29). The phosphoindependent interaction of GarA with metabolic enzymes was shown to be blocked by an intramolecular inhibition mechanism triggered by PknG/PknB-mediated GarA phosphorylation (29).

The phosphoindependent interactions of FHA domains, long believed to interact solely with phosphoproteins, is an emerging concept with few examples (29, 30). In this study we have attempted to understand the role of the previously uncharacterized FHA domain-containing protein Rv0019c and have shown its association with phosphorylated and unphosphorylated proteins. We have also provided vital clues for a possible involvement of Rv0019c in mycobacterial virulence.

TABLE 1
Primers used in the study

Primer	Sequence[a] (5′–3′)
Rv0019c F[b]	GGACGGAAAGGGATCCAGATGCAGGGGTTGGTA (BamHI)
Rv0019c R	CATCGTCGCCAGCTCGAGTCACGGGCGCCAACTC (XhoI)
19cΔT F	TACGGATCTGGATCCCCGACATTTATGCGCCGAC (BamHI)
19cΔT R	CATCGTCGCCAGCTCGAGTCACGGGCGCAACTC (XhoI)
19cΔT-R87A F	GCCGGTGTTGATCGGG**GCC**GCCGACGACTCGACCC
19cΔT-R87A R	GGGTCGAGTCGTCGGC**GGC**CCCGATCAACACCGGC
19cΔT-S101A F	GACCAGCGAACTACGCC**GCG**ACGCGGCACGCTCGGC
19cΔT-S101A R	GCCGAGCGTGCCGCGT**CGC**GGCGTAGTCGTCGGTC
19cΔT-T36A F	CCGACATTTATGCGCCG**GCC**GGCGCGGTCATGATGCG
19cΔT-T36A R	CGCATCATGACCGCGCC**GGC**CGGCGCATAAATGTCGG
19cΔT-T50A F	CCTGGCGCTGCGAGGG**GCG**CTCTTAGGCGCGCGTC
19cΔT-T50A R	GACGCGCGCCTAAGAG**CGC**CCCTCGCAGCGCCAGG
19cΔT-FHA F	CTGCGAGGGATCCTCTTAGGCGCGCGTCAGCGC (BamHI)
19cΔT-FHA R	CATCGTCGCCAGCTCGAGTCACGGGCGCAACTC (XhoI)
19cΔT-CHR F	GTATCACGCGGATCCAACAGCCGGTGTTGATCG (BamHI)
19cΔT-CHR R	CATCGTCGCCAGCTCGAGTCACGGGCGCAACTC (XhoI)
PknB F	CGCGTCGCTGGCCGGATCCGAGATAGCGCA (BamHI)
PknB R	GGCCAGTAGCTCGAGCCGCGCTAGCGGTTGAAG (XhoI)
PknBK40M F	CCGCGACGTTGCGGTC**ATG**GTGCTGGCGCGCTGATG
PknBK40M R	GATCAGCGCGCAGCAC**CAT**GACCGCAACGTCGCGG
PknB-(1–331) F	CGCGTCGCTGGCCGGATCCGAGATAGCGCA (BamHI)
PknB-(1–331) R	GGCGACCACCTCGAGCTAACGGCCCACCGAACC (XhoI)
PknB-(1–331) T171A F	AGCGGCAACAGCGTG**GCC**CAGACCGCAGCAGTGATC
PknB-(1–331) T171A R	GATCACTGCTGCGGTCTG**GGC**ACGCTGTTGCCGCT
PknB-(1–331) T173A F	AGCGGCAACAGCGTGACCCAG**GCC**GCAGCAGTGATC
PknB-(1–331) T173A R	GATCACTGCTGC**GGC**CTGGGTCACGCTGTTGCCGCT
PknB-(1–331)T171A/T173A F	CGGCAACAGCGTG**GCC**CAG**GCC**GCAGCAGTGATCG
PknB-(1–331) T171A/T173A R	CGATCACTGCTGC**GGC**CTG**GGC**CACGCTGTTGCCG
PknB-(1–331) T294 F	CACCGATGCCGAGCGG**GCC**TCGCTGCTGTCGTCTG
PknB-(1–331) T294 R	CAGACGACAGCAGCGA**GGC**CCGCTCGGCATCGGTG
PknB-(1–331) T309 F	CCTTAGCGGTCCGCGC**GCC**GATCCGCTACCACGCC
PknB-(1–331) T309 R	GGCGTGGTAGCGGATC**GGC**GCGCGGACCGCTAAGG
CAT F	AAGGATCCATATGGAGAAAAAAATCACTGGATATACCACC (BamHI)
CAT R	AAGCGGCCGCTTACGCCCCGCCCTGCCACTCATCGCAGTA (NotI)
PapA5 F	CCGTGACGAGTTGGGAATTCTGAGATGTTTCCCG (EcoR1)
PapA5 R	GACCTAACGAACGCGGCCGCCGATCGGGCTTC (NotI)
GarA F	GCGGCCAGTGAGGGATCCGGGTGACGGACATGAAC (BamH1)
GarA R	CCCGGCCAGCTCGAGGCTATCGGGTGCGCTCA (XhoI)
$MstP_{cat}$ F	CCACAAGTGGGGAATTCCCCCACCCGCTTG (EcoRI)
$MstP_{cat}$ R	CGGTCACCAGTGCGGCCGCGAATGCTCACCGTCGGCC (NotI)

[a] Restriction sites are underlined and specified in the parentheses after the sequence. Mutagenized codons are shown as bold.
[b] F, forward; R, reverse.

EXPERIMENTAL PROCEDURES

Bacterial Strains and Growth Conditions—Escherichia coli strain DH5α (Novagen) was used for cloning, and BL21(DE3) CodonPlus (Stratagene) or BL21(DE3) (Stratagene) for the expression of recombinant proteins. *E. coli* cells were grown and maintained with constant shaking (220 rpm) at 37 °C in LB medium supplemented with 100 μg/ml of ampicillin and/or 25 μg/ml of chloramphenicol, when needed.

Cloning, Expression, and Purification of Rv0019c, Its Mutants, and GarA—The *rv0019c* gene, its fragments coding for 19cΔT (Rv0019c deletion mutant devoid of N-terminal 1–30 residues), 19cFHA (Rv0019c deletion mutant comprising of FHA domain from residues 52–155), and 19cCHR (Rv0019c deletion mutant encompassing FHA domain core homology region from residues 80 to 155) and the gene encoding for *garA* were PCR amplified using *M. tuberculosis* genomic DNA as a template and the forward and reverse primers (Table 1), containing BamHI and XhoI restriction sites, respectively. The amplified products were digested with restriction enzymes, BamHI and XhoI, and ligated into vector pGEX-5X-3 (GE Healthcare), previously digested with the same enzymes to yield the plasmids listed in Table 2. The pGEX-*rv0019c*-ΔT construct was utilized for generating R87A, S101A, T36A, and T50A mutations. pGEX-*rv0019c*-ΔT was subjected to site-directed mutagenesis using the QuikChange XL Site-directed Mutagenesis kit (Stratagene) and primer pairs carrying the desired mutations (Table 1). The plasmids thus generated are listed in Table 2. The integrity of all constructs was confirmed by DNA sequencing. *E. coli* BL21-CodonPlus or BL21(DE3) cells were transformed with pGEX-5X-3 vector derivatives expressing 19cΔT, 19cFHA, 19cCHR, R87A, S101A, T36A, T50A, and GarA proteins. For overexpression, recombinant *E. coli* strains harboring the pGEX-5X-3 derivatives were used to inoculate 1000 ml of LB medium supplemented with chloramphenicol and/or ampicillin followed by incubation at 37 °C with shaking (220 rpm) until A_{600} reached 0.8. Isopropyl 1-thio-β-D-galactopyranoside was added to a final concentration of 1 mM and growth was continued for an additional 2 h at 37 °C. Cells were harvested and stored at −80 °C. Pellets were thawed on ice and resuspended in cell lysis buffer A (50 mM Tris-Cl, pH 8.0, 300 mM NaCl, 1 mM dithiothreitol, 1 mM EDTA, 1× protease inhibitor mixture (Roche Applied Science)) and lysed by sonication. The cell lysates were centrifuged at 23,430 × *g* at 4 °C for 20 min. The supernatant containing recombinant proteins was collected and incubated with glutathione-Sepharose 4B affinity resin (GE

TABLE 2
Plasmids used in this study

Plasmid	Description[a]	Ref.
pGEX-5X-3	*E. coli* vector utilized to generate GST fusion proteins and to purify GST protein	GE Healthcare
pGEX-5X-3_*rv0019c*	pGEX-5X-3 derivative used to purify GST-tagged full-length Rv0019c	This work
pGEX-5X-3_*rv0019cΔT*	pGEX-5X-3 derivative used to purify GST-tagged Rv0019c N-terminal transmembrane segment/signal peptide deletion mutant (19cΔT)	This work
pGEX-5X-3_*rv0019cFHA*	pGEX-5X-3 derivative used to purify GST-tagged Rv0019c FHA domain (19cFHA)	This work
pGEX-5X-3_*rv0019cCHR*	pGEX-5X-3 derivative used to purify GST-tagged Rv0019c core homology region (19cCHR)	This work
pGEX-5X-3_*rv0019cΔT_R87A*	pGEX-5X-3 derivative used to purify GST-tagged 19cΔT carrying R87A mutation (R87A)	This work
	pGEX-5X-3_*rv0019cΔT_S101A* pGEX-5X-3 derivative used to purify GST-tagged 19cΔT carrying S101A mutation (S101A)	This work
pGEX-5X-3_*rv0019cΔT_T36A*	pGEX-5X-3 derivative used to purify GST-tagged 19cΔT carrying T36A mutation (T36A)	This work
pGEX-5X-3_*rv0019cΔT_T50A*	pGEX-5X-3 derivative used to purify GST-tagged 19cΔT carrying T50A mutation (T50A)	This work
pGEX-5X-3_*garA*	pGEX-5X-3 derivative used to purify GST-tagged GarA (GarA)	This work
pProExHTc	*E. coli* vector used to generate His_6 fusion proteins (Invitrogen) pProExHTc_*pknB*	This work
	pProExHTc derivative used to purify His_6-tagged PknB (PknB)	
pProExHTc_*pknB_K40M*	pProExHTc derivative used to purify His_6-tagged PknB carrying K40M mutation (PknBK40M)	This work
pProExHTc_*pknB*-(1–331)	pProExHTc derivative used to purify His_6-tagged PknB cytosolic domain (PknB-(1–331))	This work
pProExHTc_*pknB*-(1–331)_*T171A*	pProExHTc derivative used to purify His_6-tagged	This work
PknB-(1–331) carrying T171A mutation (T171A)	pProExHTc_*pknB1–331_T173A* pProExHTc derivative used to purify His_6-tagged PknB-(1–331) carrying T173A mutation (T173A)	This work
pProExHTc_*pknB*-(1–331)_*T171A/T173A*	pProExHTc derivative used to purify His_6-tagged PknB-(1–331) carrying T171A and T173A mutation (T173A/T173A)	This work
pProExHTc_*pknB*-(1–331)_*T294A*	pProExHTc derivative used to purify His_6-tagged PknB-(1–331) carrying T294A mutation (T294A)	This work
pProExHTc_*pknB*-(1–331)_*T309A*	pProExHTc derivative used to purify His_6-tagged PknB-(1–331) carrying T309A mutation (T309A)	This work
pProExHTc_*papA5*	pProExHTc derivative used to purify His_6-tagged PapA5 protein (PapA5)	This work
pProExHTc_*cat*	pProExHTc derivative used to purify His_6-tagged CAT protein (CAT)	This work
pProExHTc_*mstP*$_{cat}$	pProExHTc derivative used to purify His_6-tagged MstP cytosolic domain ($MstP_{cat}$)	This work

[a] The names of purified proteins are mentioned in parentheses after vector description.

Healthcare) pre-equilibrated with buffer A. After extensive washings with buffers A and B (50 mM Tris-Cl, pH 8.0, 1 M NaCl, 1 mM dithiothreitol, 1 mM EDTA, 1 mM phenylmethylsulfonyl fluoride, and 10% glycerol) elution was carried out in elution buffer E (50 mM Tris-Cl, pH 8.5, 10% glycerol, 150 mM NaCl, and 15 mM glutathione). Fractions were run on 10% SDS-PAGE and analyzed by Coomassie staining. Pure fractions were dialyzed (20 mM Tris-Cl, pH 8.0, 10% glycerol, and 150 mM NaCl), aliquoted, and stored at −80 °C.

Cloning, Expression, and Purification of PapA5, PknB, PknBK40M, PknB-(1–331), MstP$_{cat}$*, PknB-(1–331) Threonine Mutants (Thr*^{171}*, Thr*^{173}*, Thr*$^{171/173}$*, Thr*^{294}*, and Thr*^{309}*), and E. coli Chloramphenicol Acetyltransferase (CAT)*—The genes encoding for the *papA5*, *pknB*, and *pknB*-(1–331)-*pknB* segments coding for the cytoplasmic domain (catalytic domain + juxtamembrane region, 1–331 amino acids (31)) and the $MstP_{cat}$-MstP segment coding for the cytoplasmic domain (1–300 amino acids) (31) were PCR amplified using *M. tuberculosis* genomic DNA, whereas *E. coli cat* was amplified from plasmid (pACYC) isolated from the *E. coli* BL21 CodonPlus strain, using appropriate primer pairs (see Table 1). The amplicons thus generated were digested with corresponding restriction enzymes and ligated into pProEx-HTc (Invitrogen) vector previously digested with similar enzymes. The plasmids thus constructed are mentioned in Table 2. Threonine mutations (Thr^{171}, Thr^{173}, $Thr^{171/173}$, Thr^{294}, and Thr^{309}) in pProEx-HTc-*pknB*-(1–331) and the PknBK40M mutant were generated using the QuikChange XL Site-directed Mutagenesis kit (Stratagene) and primer pairs carrying the desired mutations (Table 1). The recombinant proteins were essentially purified as described above with minor alterations. For His_6-tagged proteins, induction with isopropyl 1-thio-β-D-galactopyranoside was carried out for 12 h at 15 °C. After sonication with buffer A1 (50 mM Tris-Cl, pH 8.5, 300 mM NaCl, 5 mM β-mercaptoethanol, and 1× protease inhibitor mixture (Roche Applied Science)) PknB full-length and PknBK40M were solubilized from inclusion bodies using solubilization buffer (1.5% *N*-lauryl sarcosine, 25 mM triethanolamine, 1 mM $MgCl_2$, 1% Triton X-100, 50 mM Tris-Cl, pH 8.5, 300 mM NaCl, 5 mM β-mercaptoethanol, 1× protease inhibitor mixture (Roche Applied Science)). The supernatant obtained after centrifugation (23,430 × *g* at 4 °C for 20 min) was incubated with Ni^{2+}-nitrilotriacetic acid resin (Qiagen) previously equilibrated with buffer A1. The soluble proteins were processed as described above. Washings and elution were carried out as described above. Buffers used were B1 (50 mM Tris-Cl, pH 8.5, 1 M NaCl, 5 mM β-mercaptoethanol, 20

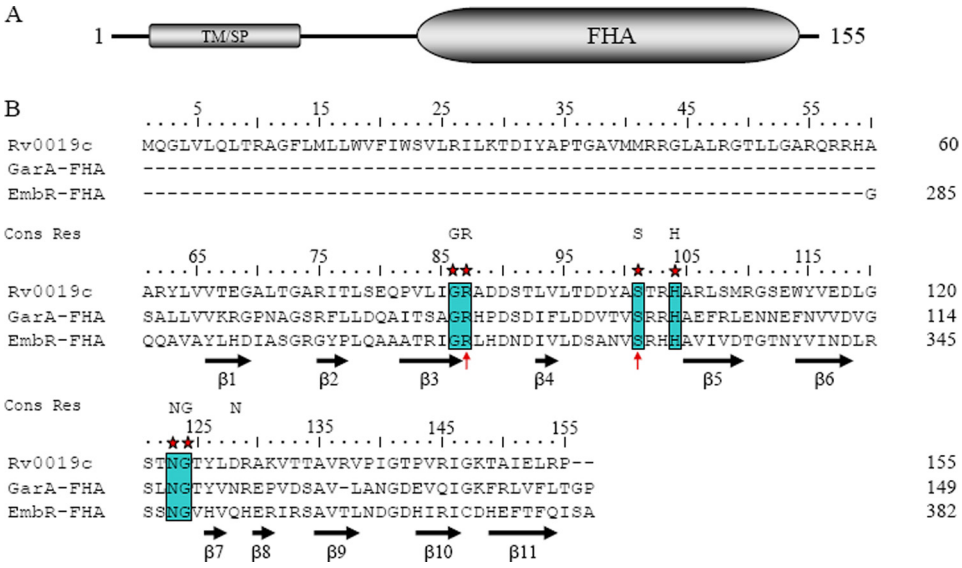

FIGURE 1. **Domain architecture of *M. tuberculosis* Rv0019c and amino acid sequence alignment with FHA domains of GarA and EmbR.** *A*, a schematic representation of Rv0019c domain organization. *TM*, *trans*-membrane region; *SP*, signal peptide. The domains of Rv0019c were predicted using Smart and Interproscan. *B*, the alignment was performed using ClustalW2. Six conserved residues in the FHA core homology region are *boxed* and marked with a *star*. The seven conserved residues found in >65% of FHA domains are shown *above* the alignment. The residues chosen for mutagenesis are indicated by an *arrow*. Secondary structural elements of EmbR (34) are shown *below* the alignment.

mM imidazole, 10% glycerol, and 1 mM phenylmethylsulfonyl fluoride) and E1 (50 mM Tris-Cl, pH 8.5, 150 mM NaCl, 10% glycerol, and 200 mM imidazole) for washings and elution, respectively.

Sandwich ELISA—ELISA was done using the method described by Lu *et al.* (32) with minor modifications. Briefly, the GST-tagged proteins were dissolved in coating buffer (0.1 M $NaHCO_3$, pH 9.2) at a concentration of 10 μg/ml and adsorbed (50 μl/well) on the surface of a 96-well ELISA plate (Maxisorb, Nunc) overnight at 4 °C. After rinsing the wells five times with wash buffer (phosphate-buffered saline, pH 7.4, 0.05% Tween 20) the reactive sites were blocked with blocking buffer (2% bovine serum albumin in wash buffer) for 2 h at room temperature. The adsorbed proteins were challenged with varying concentrations of soluble His_6-tagged proteins (50 μl/well) dissolved in blocking buffer for 1 h at room temperature. After five washes with wash buffer, the wells were treated with penta-His-horseradish peroxidase-conjugated monoclonal antibody (Qiagen) at 1:10,000-fold dilution for 1 h at room temperature. Followed by five washes, the chromogenic substrate OPD (0.4 mg/ml *o*-phenylenediamine dihydrochloride in 0.1 M phosphate/citrate buffer, pH 5) and H_2O_2 were used to visualize the interaction. After addition of stop solution (2.5 M H_2SO_4) the absorbance was read at 490 nm.

In Vitro Kinase Assay—*In vitro* kinase assays were performed with 1–2 μg of PknB, PknBK40M, PknB-(1–331), or PknB-(1–331) threonine mutants (Thr^{171}, Thr^{173}, $Thr^{171/173}$, Thr^{294}, and Thr^{309}) added separately in 15 μl of kinase buffer (20 mM PIPES, pH 7.2, 5 mM $MgCl_2$, 5 mM $MnCl_2$) with 2–4 μg of the desired protein (19cΔT, 19cFHA, 19cCHR, R87A, S101A, T36A, T50A, GST, PapA5). Reactions were started with the addition of 10 μCi of [γ-^{32}P]ATP (BRIT, Hyderabad, India) and incubated at 25 °C for 20 min. The reactions were terminated by the addition of 5× SDS sample buffer and a subsequent boiling for 5 min. Samples were resolved on 10% SDS-PAGE. Gels were dried and visualized using FLA2000 PhosphorImager (Fuji). For visualization of the phosphorylation signal on cleaved proteins, removal of recombinant tags was achieved by addition of proteases (Factor Xa (Novagen) for GST-tagged proteins and TEV for His_6-tagged proteins) after the kinase reaction had proceeded for 20 min followed by an additional incubation for 2 h at 20 °C. The reactions were stopped using SDS buffer and resolved on 15% SDS-PAGE. Likewise, for dephosphorylation of phosphorylated 19cΔT and PapA5, reactions were incubated with $MstP_{cat}$ (500 ng) for an additional 0, 1, and 30 min at 25 °C, stopped, and resolved on 10% SDS-PAGE. The signals were visualized by autoradiography.

Phosphoamino Acid Analysis—19cΔT and PapA5 were phosphorylated by PknB as mentioned above, separated by SDS-PAGE, and electroblotted onto Immobilon PVDF membrane (Millipore). The phosphorylated 19cΔT and PapA5 proteins were detected by autoradiography and the bands corresponding to γ-^{32}P-labeled substrates were excised and hydrolyzed in 6 M HCl for 1 h at 110 °C. The hydrolyzed samples containing liberated phosphoamino acids were lyophilized and redissolved for phosphoamino acid analysis by two-dimensional thin layer electrophoresis as described (33).

Immunoblotting—To determine the phosphorylation status of recombinant CAT and PapA5 by Western blot analysis, the freshly purified proteins were resolved by SDS-PAGE along with positive (PknB for anti-phosphothreonine) and negative (GST) controls and transferred onto nitrocellulose membrane (Bio-Rad). After overnight blocking of membrane with 3% bovine serum albumin in PBST (phosphate-buffered saline, pH 7.2, 0.1% Tween 20), the blot was incubated for 1 h at room temperature with antibodies directed against phosphoserine or phosphothreonine (Invitrogen) dissolved in PBST at 1:10,000 dilution. Followed by five washes the blot was incubated for 1 h at room temperature with anti-rabbit horseradish peroxidase polyclonal antibody (Sigma) dissolved in PBST (1:10,000 dilution). After five washes the blots were developed using ECL Plus kit (GE Healthcare) according to the manufacturer's instructions.

RESULTS

Domain Architecture and Genomic Organization of Rv0019c—Rv0019c is a small 155-amino acid protein encompassing a predicted N-terminal transmembrane domain/signal peptide and a C-terminal FHA domain occupying the majority of the protein (Fig. 1*A*). Amino acid sequence alignment of Rv0019c with

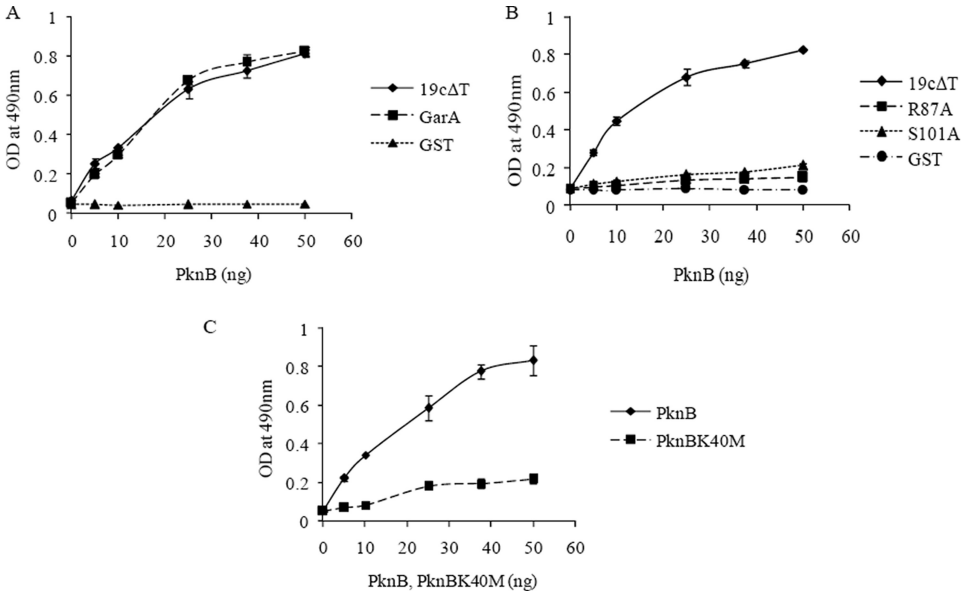

FIGURE 2. ***In vitro* interaction of 19cΔT and its mutants with PknB.** *A*, GST-tagged 19cΔT, GarA (positive control), and GST alone (negative control) were immobilized (500 ng/well) on the surface of the microtiter plate and challenged with increasing concentrations of His_6 PknB (0–50 ng) in solution. As shown, 19cΔT readily formed a complex with PknB, and binding was comparable with the GarA-PknB interaction. The negative control GST failed to interact with PknB even at higher kinase concentrations. *B*, mutation of the conserved Arg^{87} and Ser^{101} abrogated the 19cΔT-PknB interaction. *C*, PknBK40M, the autophosphorylation deficient mutant of PknB, elicited a weak binding with 19cΔT as compared with PknB. The *error bars* are the S.D. of the triplicate ELISA OD readings.

FHA domains of mycobacterial proteins with known x-ray or NMR structure (34, 29) shows the conservation of six of the seven hallmark residues for FHA domains in Rv0019c (Fig. 1*B*). Of the six FHA domain-containing proteins encoded in the *M. tuberculosis* genome, four have been characterized and the conserved residues in the FHA domains have been shown to play a crucial role in their interaction with autophosphorylated STPKs (24, 35, 36). In the *M. tuberculosis* genome, Rv0019c resides within a cluster of genes encoding for essential STPKs PknA and PknB, morphogenic proteins PbpA and RodA, and the only identified Ser/Thr phosphatase MstP. The orthologs of Rv0019c and PknB show strong conservation and display similar genomic organization in various members of actinomycetales (supplemental Fig. S1). The ubiquitous presence of Rv0019c orthologs along with those of PknB hints at a role of *M. tuberculosis* Rv0019c in PknB-mediated signaling events through an inevitable interaction between the two proteins mediated by the Rv0019c FHA domain.

In Vitro Interaction of Rv0019c with PknB—To determine whether Rv0019c develops a direct physical contact with PknB, interaction studies were carried out using sandwich ELISA as described under "Experimental Procedures." Recombinant N-terminal GST-tagged or His_6-tagged Rv0019c was invariably localized to inclusion bodies during purification from *E. coli* (data not shown). A deletion mutant lacking the predicted N-terminal transmembrane region/signal peptide (1–30 amino acids) was generated to facilitate its purification from soluble fraction. As shown in Fig. 2*A*, robust interaction was observed between the recombinant GST-tagged deletion product of Rv0019c (19cΔT) and purified autophosphorylated His_6-tagged PknB (0–50 ng). Notably, PknB is capable of catalyzing autophosphorylation during its expression in *E. coli* (37) and hence the autophosphorylated purified kinase was used directly for interaction studies. GST alone acted as a negative control, whereas GarA, a characterized FHA domain containing the interaction partner of PknB was included as a positive control (Fig. 2*A*). As mentioned above, the FHA domain-containing proteins primarily form contact with their phosphorylated targets through conserved residues in their FHA domains. To ensure that the observed 19cΔT-PknB interaction was mediated by the FHA domain of 19cΔT, the conserved residues in its FHA domain core homology region (Arg^{87} and Ser^{101}) were mutagenized to alanine by site-directed mutagenesis. When compared with 19cΔT, FHA domain mutants 19cΔTR87A (R87A) and 19cΔTS101A (S101A) displayed a significant reduction in their capacity to interact with PknB (Fig. 2*B*). Alternatively, the PknB kinase-dead mutant (PknBK40M), deficient of autophosphorylation, also exhibited lower binding affinity with 19cΔT (Fig. 2*C*). Because PknBK40M was purified as an unphosphorylated protein from *E. coli* (Fig. 5*E*), we expected a total loss of interaction with 19cΔT, the implication of the basal contact thus observed is discussed in later sections.

In Vitro Phosphorylation of Rv0019c by PknB—An interaction between a kinase and a FHA domain-containing protein does not necessarily lead to the phosphorylation of the latter. Recently Molle *et al.* (38) demonstrated the lack of PknH-mediated phosphorylation of EmbR2, an FHA domain containing EmbR homolog, albeit an efficient interaction of EmbR2 with phosphorylated peptides derived from PknH. Therefore, the ability of proximally located PknB to act as a "true" Rv0019c kinase was tested. When incubated in the presence of PknB and [γ-^{32}P]ATP, phosphotransfer was evident on 19cΔT (Fig. 3*A*). No incorporation of radiolabel was observed on 19cΔT when incubated alone or in the presence of PknBK40M thereby validating a PknB-specific phosphorylation of 19cΔT (Fig. 3*A*). To ensure that the observed phosphorylation is localized on the native protein and not on the recombinant GST tag, the fusion tag was removed with Factor Xa protease and phosphorylation was confirmed to be specifically localized on the released 19cΔT protein (data not shown). Furthermore, in agreement with the interaction studies on FHA domain mutants (R87A and S101A) with PknB, both mutants were labeled to a much lesser extent as compared with 19cΔT under similar reaction conditions (Fig. 3*B*). As mentioned previously, Rv0019c is encoded within a cluster of genes comprising Ser/Thr phosphatase MstP. Therefore, it was pertinent to believe that 19cΔT would be targeted by MstP for dephosphorylation. As expected the phosphorylation of 19cΔT was completely reversed by MstP (Fig. 3*C*).

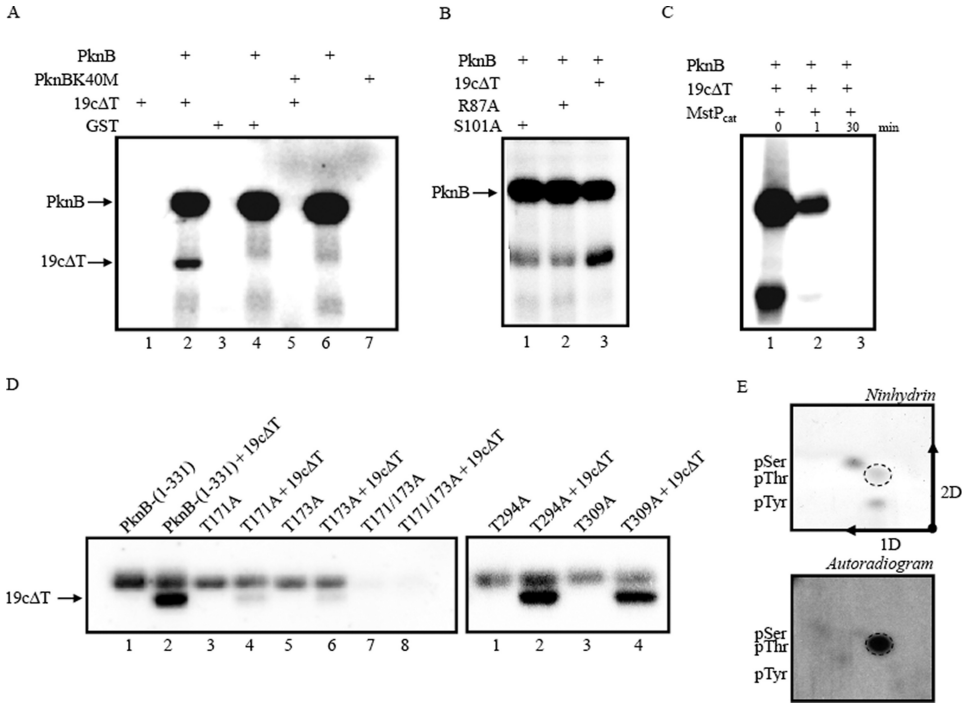

FIGURE 3. ***In vitro* phosphorylation of Rv0019c by PknB.** *A*, 2 μg of purified PknB or PknBK40M was incubated with 4 μg of 19cΔT in the presence of [γ-^{32}P]ATP for 20 min at 25 °C. The reactions were run on SDS-PAGE, and the gel was autoradiographed after drying. As shown, transphosphorylation on 19cΔT was visible only in the presence of PknB (*lane 2*). GST was used as a negative control (*lane 4*). *B*, comparative *in vitro* phosphorylation of 19cΔT FHA domain mutants R87A (*lane 2*) and S101A (*lane 1*) with 19cΔT (*lane 3*). *C*, dephosphorylation of 19cΔT. 2 μg of PknB was incubated with 4 μg of 19cΔT in the presence of [γ-^{32}P]ATP for 20 min at 25 °C. After the phosphorylation reaction, 500 ng of MstP$_{cat}$ was added and reactions were further incubated for the indicated times. The signals were visualized by autoradiography. *D*, the phosphorylatable threonine residues were mutagenized in a smaller construct of PknB, PknB-(1–331). Diminished phosphorylation of 19cΔT by T171A (*lane 4*) and T173A (*lane 6*) clearly indicated the necessity of Thr^{171} and Thr^{173} residues for the phosphorylation of 19cΔT. *E*, analysis of the phosphoamino acid content of 19cΔT phosphorylated by PknB. Amino acid standards, phosphoserine (*pSer*), phosphothreonine (*pThr*), and phosphotyrosine (*pTyr*) were added in the radiolabeled sample and visualized by ninhydrin staining (*upper panel*) prior to autoradiography (*lower panel*). The labeled Thr(P) and its corresponding standard are *encircled*.

Because the 19cΔT-PknB interaction and the consequent 19cΔT phosphorylation was primarily dependent on the FHA domain of 19cΔT and FHA domains are known phosphothreonine interaction modules, we next mutagenized the four phosphorylatable threonine residues (Thr^{171}, Thr^{173}, Thr^{294}, and Thr^{309}) in PknB (39). Thr^{171} and Thr^{173} residues are situated in the activation loop of PknB, whereas Thr^{294} and Thr^{309} reside in the juxtamembrane region. For ease of purification, the threonine mutations were created in a smaller construct of PknB encompassing the catalytic domain and the linker juxtamembrane region (1–331 amino acids) yielding a soluble protein (31). When compared with wild type PknB-(1–331), the T171A and T173A mutants displayed weak activity toward 19cΔT, whereas the phosphotransfer on 19cΔT by T294A and T309A mutants was comparable with that of wild type PknB-(1–331) (Fig. 3*D*). These results clearly indicated at the necessity of threonine residues (Thr^{171} and Thr^{173}) in the activation loop of PknB for effective phosphorylation of 19cΔT. The activation loop threonine residues were previously shown to be critical for the phosphorylation of GarA by PknB (40), whereas similar residues in PknH played no role in its interaction with the FHA domain containing protein EmbR (34).

We next tried to analyze the nature of the amino acid labeled by PknB on 19cΔT and found that 19cΔT was exclusively phosphorylated on threonine residue(s) following incubation with PknB in the presence of [γ-^{32}P]ATP (Fig. 3*E*). In conclusion, 19cΔT phosphorylation on threonine residue(s) by PknB was found to be dependent on a fully functional activation loop of PknB and the FHA domain of 19cΔT.

Identification of the Phosphorylation Site in 19cΔT—Identification of phosphorylation sites in the substrate aids gained mechanistic insight into the complex signal transduction cascade operational within the cell. To determine the target site(s) of PknB in 19cΔT, two N-terminal deletion mutants of 19cΔT were created: one comprised of residue 52–155 constituting the predicted functional FHA domain (19cFHA) and the other encompassing residue 80–155 constituting the FHA domain core homology region (19cCHR) (Fig. 4*A*). To determine whether the deletion mutants thus created retain their functional integrity, interaction studies were carried out with His$_6$ PknB. As shown in Fig. 4*B*, 19cFHA readily formed a complex with PknB, whereas, 19cCHR and PknB showed no significant physical association. The observation was in agreement with previous studies emphasizing at the role of residues beyond the FHA core homology region in maintaining the structural and functional integrity of the FHA domain (10–12). 19cFHA was then subjected to the phosphorylation assay with PknB in the presence of [γ-^{32}P]ATP. Although PknB labeled 19cΔT, no phosphotransfer was observed on 19cFHA (Fig. 4*C*). A faint signal on 19cFHA could only be observed after a prolonged exposure (data not shown). Because 19cFHA represented a functional unit with an intact capacity to interact with PknB (Fig. 4*B*), 19cΔT-like radiolabeling was expected. The lack of phosphorylation of 19cFHA by PknB clearly pointed out the presence of a major phosphorylation site N-terminal to 19cFHA. Sequence analysis showed the presence of two threonine residues (Thr^{36} and Thr^{50}) within the motif 31–51 as the putative target sites of PknB (Fig. 4*D*). Both threonine residues were substituted to alanine using site-directed mutagenesis. Because point mutations may lead to structural perturbations in a protein, the mutants were subjected to interaction studies with the kinase to ensure that they retained functional integrity. The interaction of T36A and T50A with PknB was comparable with that of the PknB-19cΔT interaction (data not shown), hence, the mutants were subjected to phosphorylation assays with PknB. As shown in Fig. 4*E*, a substantial loss of phosphotransfer was observed on T36A with a minor phospholabeling

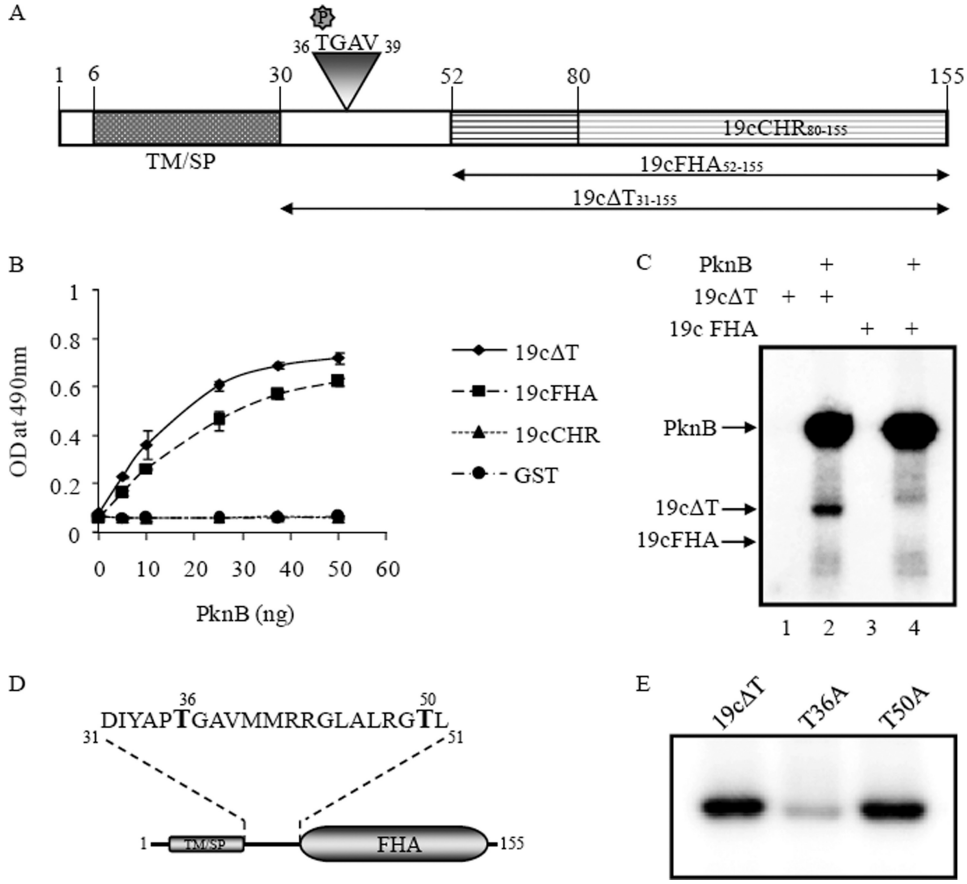

FIGURE 4. **Identification of phosphorylation site in 19cΔT.** *A*, a representation of Rv0019c showing the deletion mutants used in the study. 19cFHA and 19cCHR were created to map the phosphorylation site, identified as Thr[36] in the motif upstream of functional FHA domain (19cFHA). *B*, ELISA to determine functional integrity of deletion mutants 19cFHA and 19cCHR. 19cΔT, 19cFHA, 19cCHR, and GST (500 ng/well) were immobilized and challenged with increasing concentrations of His_6-PknB in solution. The *error bars* are the S.D. of the triplicate ELISA OD readings. *C*, similar concentrations (4 μg) of 19cΔT and 19cFHA were incubated with 2 μg of PknB in the presence of [γ-^{32}P]ATP. Under similar reaction conditions, PknB failed to radiolabel 19cFHA (*lane 4*). *D*, schematic representation of putative phosphorylation sites in the upstream region of the functional FHA domain (19cFHA). *E*, similar concentrations of 19cΔT, T36A, and T50A (4 μg) were incubated with 2 μg of PknB in the presence of [γ-^{32}P]ATP. After a prolonged exposure of 2 days, only a faint signal was observed on the T36A mutant.

observed only on prolonged exposure. Thus, threonine at position 36 was identified as the major phosphorylation site in 19cΔT.

Identification of a 19cΔT Interacting Protein from E. coli—By purification of 19cΔT and its aforementioned deletion mutants from *E. coli*, we observed a reproducible and specific co-purification of *E. coli* proteins corresponding to 50 and 25 kDa with 19cΔT and 19cFHA (Fig. 5, *A* and *B*). Interestingly, similar *E. coli* proteins failed to co-purify with the functionally inactive deletion mutant 19cCHR, FHA domain mutants R87A and S101A, and GST alone. Therefore it was tempting to speculate that the co-purified proteins were specific interaction partners of 19cΔT and that co-purification was dependent on the functional FHA domain of 19cΔT. The co-purified *E. coli* proteins corresponding to 25 and 50 kDa were identified by mass spectrometry as *E. coli* CAT. CAT is a bacterial enzyme that confers resistance to antibiotic chloramphenicol (41). Because CAT exists as a trimeric protein (41), the band corresponding to 50 kDa probably represented the SDS stable dimeric subunit and the one at 25 kDa was the dissociated monomer. To ascertain that the observed 19cΔT FHA domain specific pulldown of CAT was mimicked *in vitro*, *E. coli* CAT was expressed and purified as a recombinant His_6-tagged protein (CAT) and interaction studies were carried out with 19cΔT and its mutants. As shown in Fig. 5*C*, CAT displayed a robust interaction with 19cΔT and 19cFHA, whereas no interaction was evident between CAT and 19cCHR. Furthermore, in agreement with the copurification results, FHA domain mutants R87A and S101A failed to interact with CAT *in vitro* (Fig. 5*D*). Thus, like the PknB-19cΔT interaction, the CAT-19cΔT interaction was also found to be dependent on the functional FHA domain of 19cΔT.

Because 19cΔT and its mutants displayed a strikingly similar interaction pattern with PknB and CAT, we argued that CAT purified from *E. coli* could possibly be a phosphorylated protein. To test the hypothesis, recombinant CAT was analyzed for its phosphorylation status using anti-phosphothreonine/serine antibodies. As shown in Fig. 5*E*, CAT was found to be phosphorylated on both threonine and serine residues, thus providing a possible explanation for the observed 19cΔT-CAT interaction. Because, *E. coli* CAT was found to be phosphorylated on threonine residue(s) and FHA domains are phosphothreonine binding modules, we next suspected that the co-purification of *E. coli* CAT with 19cΔT could be due to the high affinity of a FHA domain for a phosphoprotein. To rule out the possibility of a promiscuous interaction, GST-GarA was purified under similar purification conditions and subjected to interaction studies with CAT. Interestingly, no interaction was observed between purified GarA and CAT (Fig. 5*F*), providing conclusive evidence for the specificity of the CAT-19cΔT interaction.

19cΔT Interacts with PapA5, the Structural Homolog of E. coli CAT in M. tuberculosis—The FHA domain-specific interaction of CAT with 19cΔT and the tantalizing specificity prompted us to investigate for a sequence homolog of *E. coli* CAT in *M. tuberculosis*. To our surprise, no sequence homolog was identified in *M. tuberculosis* when the *E. coli* CAT sequence was used as a query to search the *M. tuberculosis* genome. However, we could find a report on PapA5, a polyketide-associated protein with acetyltransferase activity, sharing considerable structural similarity with *E. coli* CAT (42). *M. tuberculosis* PapA5 is involved in the synthesis of virulence enhancing lipids and is a

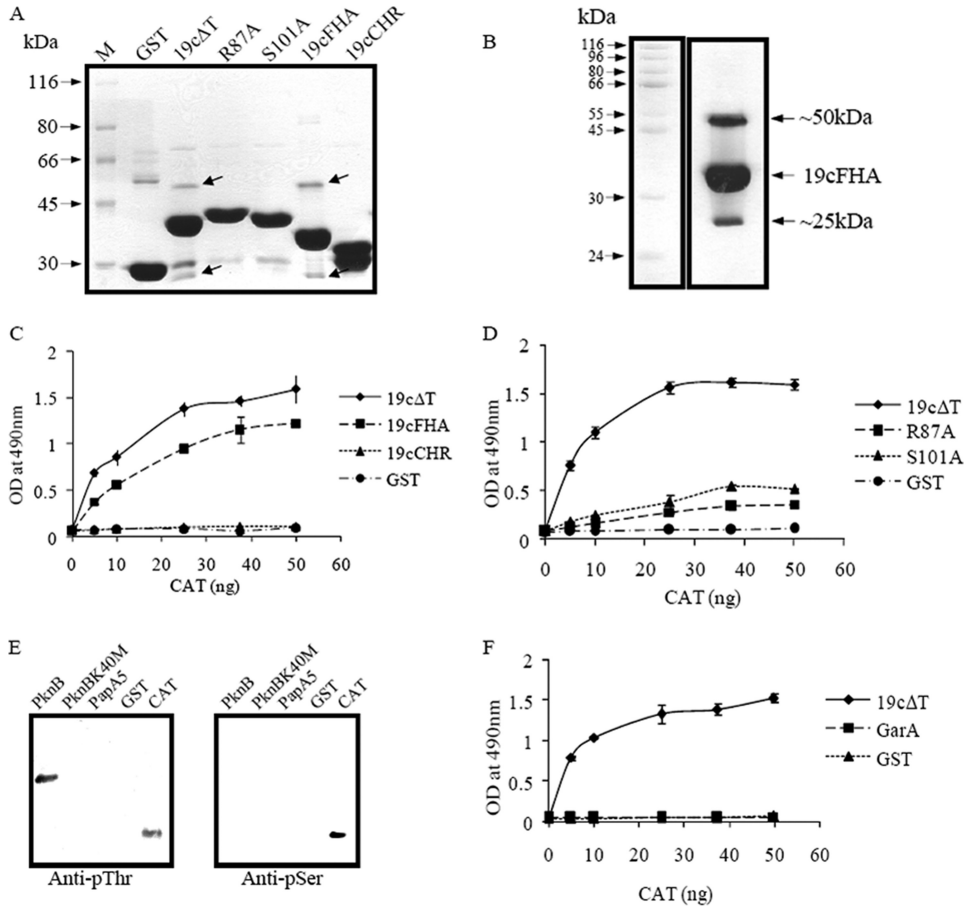

FIGURE 5. **Identification of a 19cΔT interacting protein from *E. coli*.** *A*, GST-tagged 19cΔT, R87A, S101A, 19cFHA, 19cCHR, and GST proteins were overproduced and purified from *E. coli*. Equal concentrations (15 μg) of the above mentioned proteins were separated by SDS-PAGE and stained with Coomassie Blue. 19cCHR was purified as a doublet. Proteins corresponding to ~25 and ~50 kDa reproducibly copurified with 19cΔT and 19cFHA are shown by *arrows*. *B*, Coomassie-stained gel showing the characteristic copurification of *E. coli* CAT with freshly purified 19cFHA. *C*, *E. coli* CAT was overproduced and purified as a recombinant His_6-tagged protein and allowed to interact *in vitro* with immobilized 19cΔT, its deletion mutants 19cFHA and 19cCHR, and GST (500 ng/well). *D*, interaction of immobilized FHA domain mutants R87A and S101A (500 ng/well) with CAT in solution. *E*, 2 μg of freshly purified proteins (PknB, PknBK40M, PapA5, GST, and CAT) were resolved on SDS-PAGE and transferred onto nitrocellulose membrane and probed with anti-phosphoserine (*right panel*) or anti-phosphothreonine (*left panel*) antibody as described under "Experimental Procedures." *F*, interaction of CAT with immobilized 19cΔT, GarA, and GST (500 ng/well). *pSer*, phosphoserine; *pThr*, phosphothreonine. The *error bars* are the S.D. in the triplicate ELISA OD readings.

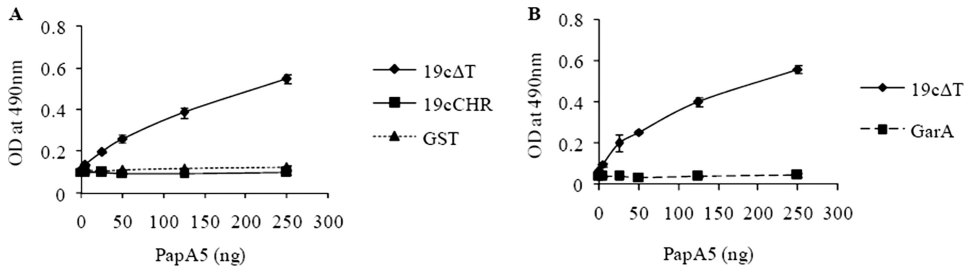

FIGURE 6. **Interaction of PapA5 with 19cΔT.** *A*, *M. tuberculosis* PapA5 was cloned, overproduced, and purified as a His_6-tagged protein using Ni^{2+}-nitrilotriacetic acid resin as described under "Experimental Procedures." 19cΔT, 19cCHR, and GST were immobilized (500 ng/well) on the surface of a microtiter plate and treated with increasing concentrations of His_6-tagged PapA5 (0–250 ng). *B*, relative interaction of PapA5 with immobilized GarA and 19cΔT. The *error bars* are the S.D. in the triplicate ELISA OD readings.

suspected membrane protein (43, 44). Although *E. coli* CAT and *M. tuberculosis* PapA5 share only 12% sequence identity, the regions of structural similarity shared between the two proteins stretch beyond the acetyltransferase domain and span 127 amino acid residues at the 3.9 Å root mean square deviation (42). To test the possibility of a PapA5–19cΔT interaction, PapA5 was expressed and purified as a recombinant His_6-tagged protein and allowed to interact with 19cΔT. As shown in Fig. 6*A*, an interaction was apparent between immobilized 19cΔT and PapA5 (0–250 ng) in solution, whereas the functionally inactive deletion mutant 19cCHR and GST failed to form a complex with PapA5 (Fig. 6*A*). The specificity of interaction was further ascertained by incubating GarA with PapA5. Because GarA displayed no affinity for PapA5 (Fig. 6*B*), the polyketide-associated protein with a structural similarity with *E. coli* CAT was identified as a specific interaction partner of 19cΔT.

PapA5–19cΔT Interaction Is Not Dependent on the Functional FHA Domain of 19cΔT—Although PapA5 displayed an affinity for 19cΔT, the complex was formed at a significantly higher concentration of PapA5 (0–250 ng) when compared with CAT (0–50 ng) in CAT-19cΔT interaction under similar reaction conditions. Because, PapA5 was purified as an unphosphorylated protein from *E. coli* (Fig. 5*E*), we reasoned that in the absence of phosphorylation and hence the phosphointeraction motif for the FHA domain of 19cΔT, the 19cΔT-PapA5 complex would be loosely held by hitherto unidentified interactions. To investigate the nature of these interactions and determine the role of the FHA domain, if any, in the phosphoindependent contact of 19cΔT with PapA5, we utilized FHA domain mutants R87A and S101A. As shown in Fig. 7*A*, the 19cΔT-PapA5 complex was unaffected by the S101A mutation, whereas association was apparently reduced when Arg^{87} was mutagenized. The results were in stark contrast from those obtained from 19cΔT-PknB and 19cΔT-CAT interaction studies, where the mutation of Arg^{87} and Ser^{101} residues abrogated the complex formation (see Figs. 2*B* and 5*D*). These results prompted us to investigate the role of residues N-terminal of the functional FHA domain in 19cΔT-PapA5 complex formation. To our surprise, the deletion mutant 19cFHA, encompassing the func-

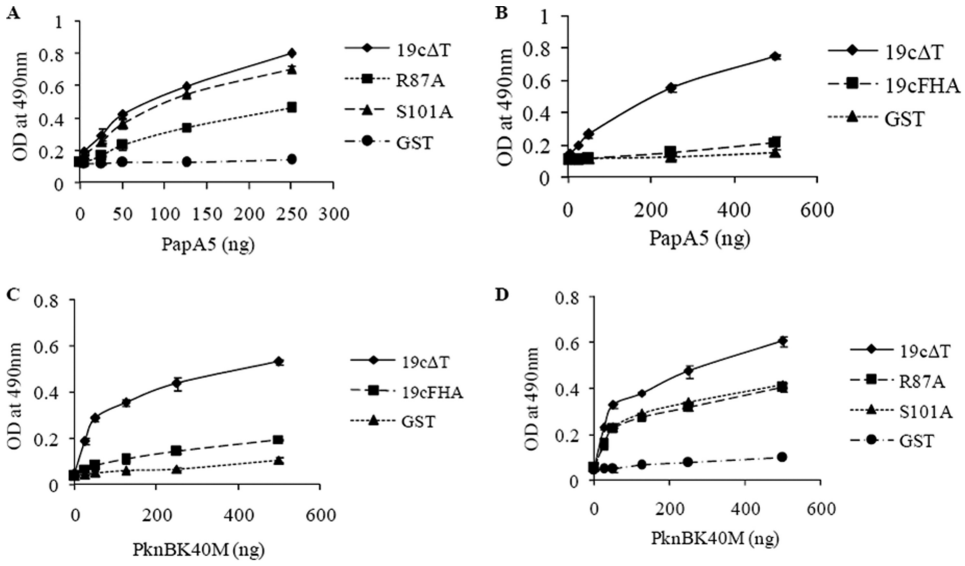

FIGURE 7. **Phosphoindependent interaction of 19cΔT with PapA5 and PknBK40M.** *A*, 19cΔT, R87A, S101A, and GST (500 ng/well) were adsorbed on the surface of a microtiter plate and incubated with increasing concentrations of His_6-tagged PapA5 in solution. The graph shows the relative interaction of PapA5 with 19cΔT FHA domain mutants and 19cΔT. Note that the 19cΔT-PapA5 interaction is unaffected by mutation of the conserved residue Ser^{101}, thus indicating a differential mode of interaction. *B*, interaction of 19cFHA (500 ng/well) with PapA5. The deletion of residues 31–51 (19cFHA) abrogates the 19cΔT-PapA5 interaction. *C*, interaction of PknBK40M with immobilized 19cFHA (500 ng/well) shows the necessity of residues 31–51 for efficient interaction of PknBK40M with 19cΔT. *D*, interaction of PknBK40M, the autophosphorylation deficient mutant of PknB, with immobilized 19cΔT FHA domain mutants (500 ng/well). The *error bars* are the S.D. in the triplicate ELISA OD readings.

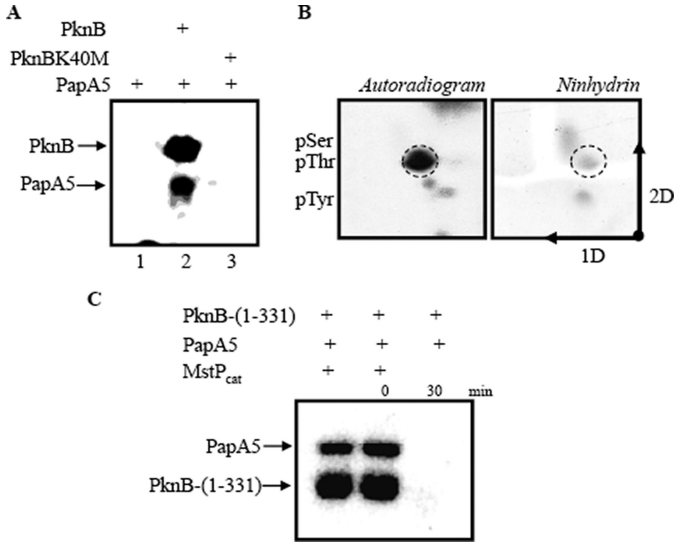

FIGURE 8. **Reversible phosphorylation of PapA5 by the PknB-MstP kinase phosphatase pair.** *A*, 2 μg of purified PknB or PknBK40M was incubated with 4 μg of PapA5 in the presence of [γ-^{32}P]ATP for 20 min at 25 °C. The reactions were stopped by the addition of 5× sample buffer and heated for 5 min at 100 °C. The samples were subsequently run on SDS-PAGE and the gel was dried and autoradiographed. PknB efficiently phosphorylated PapA5 (*lane 2*), whereas the kinase-dead mutant, PknBK40M, was unable to incorporate phospholabel on PapA5 (*lane 3*). *B*, analysis of phosphoamino acid content of PapA5 phosphorylated by PknB. The labeled Thr(P) and its corresponding standard are *encircled*. *C*, to carry out dephosphorylation of PapA5, 2 μg of PknB-(1–331) was incubated with 4 μg of PapA5 in the presence of [γ-^{32}P]ATP for 20 min at 25 °C. After the phosphorylation reaction, 500 ng of MstP$_{cat}$ was added and reactions were further incubated for the indicated times. The signals were visualized by autoradiography.

tional FHA unit and devoid of residues 31–51, was unable to form a complex with PapA5 (Fig. 7*B*). The result was rather unexpected because 19cFHA was capable of forming a high affinity complex with PknB and CAT (see Figs. 4*B* and 5*C*). From the results obtained from interaction studies on PapA5 with 19cΔT deletion mutants we concluded that in the absence of phosphorylation on the target protein (PapA5), 19cΔT interacts primarily through residues upstream of the functional FHA domain (31–51), whereas the FHA domain acts cooperatively to hold the complex. The hypothesis was further supported by the observation that the previously observed phosphoindependent basal interaction of 19cΔT with PknBK40M was substantially affected by deletion of residues from 31 to 51 (Fig. 7*C*). Additionally, as seen for the 19cΔT-PapA5 interaction, the mutation of conserved residues in the FHA domain did not completely abrogate the interaction but had a cooperative role to play in PknBK40M-19cΔT complex formation (Fig. 7*D*).

PapA5 Is a Substrate of PknB—As shown above, PapA5 and PknBK40M displayed a strikingly similar interaction pattern with 19cΔT and its mutants. Also, *E. coli* CAT, the structural homolog of PapA5, was identified as a phosphorylated protein. Therefore, it was pertinent to believe that PapA5 could also be modified by a similar post-translational modification. To test the same, we carried out phosphorylation reactions where PapA5 was incubated with PknB in the presence of [γ-^{32}P]ATP. As speculated, PapA5 was efficiently phosphorylated by PknB (Fig. 8*A*) and no incorporation of radiolabel was observed when PapA5 was incubated alone or in the presence of PknBK40M, thereby validating a PknB-specific phosphorylation of PapA5 (Fig. 8*A*). The recombinant fusion tag was removed with TEV protease and the phospholabel was confirmed to be specifically localized on the released PapA5 protein (data not shown). Furthermore, the released PapA5 was found to be exclusively phosphorylated on threonine residue(s) (Fig. 8*B*) as analyzed by two-dimensional thin layer electrophoresis. Because regulation of signaling proteins by reversible phosphorylation is a common theme in signal transduction, we next questioned whether PknB-mediated PapA5 phosphorylation could be reversed by Ser/Thr phosphatase MstP. As shown in Fig. 8*C*, MstP completely dephosphorylated PapA5 in a time-dependent manner, thereby reversing the kinase-mediated signaling. Thus, PapA5 was shown to be reversibly modified by the PknB-MstP kinase phosphatase pair.

DISCUSSION

In this report we show that the FHA domain-containing protein Rv0019c interacts with autophosphorylated cognate kinase PknB primarily through the conventional phosphopeptide binding region and is consequentially phosphorylated at its

N-terminal Thr^{36} residue by the STPK. In addition to Rv0019c-phosphoprotein interactions we also demonstrate the phosphoindependent interactions of Rv0019c. *M. tuberculosis* PapA5 is identified as an interaction partner of Rv0019c and the phosphoindependent interaction of Rv0019c with recombinant unphosphorylated PapA5 is shown to be primarily mediated by residues N-terminal to the Rv0019c FHA domain. Thus, the N-terminal interaction motif is identified as a novel phosphoindependent binding surface distinct from the previously identified phosphoindependent binding regions located on the FHA domain. Finally, PapA5 is shown to undergo reversible phosphorylation by the PknB-Mstp kinase-phosphatase pair. Therefore, this study provides a framework for further investigations on a seemingly important functional linkage between essential STPK PknB and PapA5, a protein crucial for mycobacterial virulence.

In Vitro Interaction and Subsequent Phosphorylation of Rv0019c by Cognate Kinase PknB on Thr^{36} Residue—FHA domains respond to threonine phosphorylation and a protein encompassing the FHA domain can indisputably be placed into the scheme of STPK-mediated signaling. FHA domains physically interact with target phosphopeptide through the conserved residues located in the core of the FHA domain structural scaffold (14). Among the five highly conserved residues, Arg located in the loop connecting the $\beta3/\beta4$ strand and Ser of the $\beta4/\beta5$ loop (similar to Arg^{70} and Ser^{85} in *Saccharomyces cerevisiae* $Rad53^{FHA1}$) form direct contact with the Thr(P) residue, whereas other conserved residues either interact with the phosphopeptide backbone or form a structural framework for peptide display (14). *M. tuberculosis* Rv0019c is solely comprised of the FHA domain, and sequence analysis shows the conservation of critical residues in its FHA domain. Of the conserved residues (Gly^{86}, Arg^{87}, Ser^{101}, His^{104}, Asn^{123}, and Gly^{124}) Arg^{87} of the $\beta3/\beta4$ loop and Ser^{101} of the $\beta4/\beta5$ loop were chosen for mutagenesis, because the mutation of residues similar to conserved glycine and histidine was reported to cause structural perturbations in the FHA domain (45) and was thus unsuitable for determining FHA domain function. The results clearly showed that the conserved Arg and Ser of Rv0019c were essential for its interaction with cognate kinase PknB, whereas the mutation of Arg^{87} was seemingly more detrimental for the 19cΔT-PknB interaction.

The interaction of PknB with 19cΔT resulted in phosphorylation of the latter, with the label localized solely on the threonine residue. Deletion mutants comprising the FHA domain core homology region (19cCHR, residues 80–155) and FHA domain (19cFHA, residues 52–155) were created and Thr^{36} situated in the TGAV motif upstream of FHA domain was identified as the major phosphorylation site in 19cΔT. Interestingly, the phosphorylation sites identified in GarA were also shown to be localized in the N-terminal region preceding the FHA domain. Thr^{21} and Thr^{22} situated in the conserved Thr^{21}-Thr^{22}-Ser-Val-Phe motif were reported to be targeted by PknG and PknB, respectively, in mutually exclusive phosphorylation events (28, 40). The phosphorylation of Thr residues triggered an intramolecular association of the N-terminal segment with the C-terminal FHA domain resulting in the inhibition of regulatory activities of GarA on its downstream interaction partners (29, 46). Because Rv0019c and GarA share an apparently similar C-terminal FHA domain organization and are both phosphorylated at N-terminal segments, there exists a possibility that Rv0019c could also be regulated by a similar intramolecular autoinhibition mechanism. Although for such an intramolecular interaction to happen the flexibility of the N-terminal segment seems to be a pre-requisite, which is unlikely for Rv0019c because of the presence of an N-terminal transmembrane segment. It would therefore be interesting to determine the effect of 19cΔT phosphorylation on its structure and its interaction with target proteins. The same could not be experimentally verified due to repeated precipitation of Rv0019c at higher concentrations needed to obtain assayable quantities of phosphorylated protein, and unusually strong affinity of PknB for Rv0019c, resulting in interference of His_6 PknB in ELISA reactions (data not shown). Nevertheless, our results have established that Rv0019c is a bona fide member of the FHA domain family and is modified at Thr^{36} by cognate kinase PknB.

E. coli CAT Interacts with 19cΔT in a FHA Domain-dependent Manner—Chloramphenicol acetyltransferase is a bacterial enzyme responsible for catalyzing covalent modification of antibiotic chloramphenicol by transferring an acetyl group from acetyl-CoA to the primary hydroxyl of chloramphenicol rendering the antibiotic inactive (41). The pulldown of *E. coli* CAT with 19cΔT during its purification from *E. coli* was rather fascinating because the same protein failed to copurify with the functionally inactive and FHA domain mutants of 19cΔT. The pulldown of CAT with 19cΔT is reminiscent of the copurification of 14-3-3 proteins with serotonin *N*-acetyltransferase. 14-3-3 protein interacts with serotonin *N*-acetyltransferase in a phosphorylation dependent manner (47, 48). Interestingly, our results showed that recombinant CAT was purified as a phosphorylated protein and readily formed a complex with 19cΔT and its functionally active mutant 19cFHA *in vitro*. Furthermore, we suspected the specificity of the CAT-19cΔT interaction and addressed it by showing that CAT failed to form a complex with the FHA domain-containing protein GarA. Additionally, during the purification of other mycobacterial FHA domain-containing proteins, we did not observe *E. coli* CAT co-purification (data not shown), providing further evidence for the specificity of CAT-19cΔT interaction. Of note, while carrying out interaction studies with CAT we observed that the CAT-19cΔT interaction was unusually strong. Such an interaction can possibly be explained either by the presence of an optimal binding motif for the Rv0019c FHA domain in *E. coli* CAT or by recognition of additional structural features in CAT by 19cΔT. Notably, the majority of the eukaryotic FHA domain-containing proteins have been shown to recognize a short stretch (Thr(P) −4 to Thr(P) +3) in the target peptide and are primarily grouped on the basis of their specificity for the residue at the Thr(P) +3 position (6, 15). One of the few exceptions, the Ki67-FHA domain recognizes the extended surface (44-residue stretch) on the target nucleolar protein NIFK (49) forming an exceptionally high affinity complex. Determination of the nature of the 19cΔT-CAT interaction can assist in identification of novel interaction partners of Rv0019c in *M. tuberculosis* bearing similar structural features.

Rv0019c Interacts with PapA5, the Structural Homolog of E. coli CAT, through the N-terminal Residues Preceding the FHA Domain—M. tuberculosis PapA5 is an acyltransferase bearing structural similarity with *E. coli* CAT (42). In the *M. tuberculosis* genome, the gene encoding for PapA5 is situated in a cluster of genes implicated in the biosynthesis of PDIMs, the virulence enhancing lipids (22). PapA5 catalyzes the final step in PDIM biosynthesis by mediating the direct transfer of mycocerosic acid synthase-bound mycocerosic acids onto the pthiocerols by forming direct physical contact with the mycocerosic acid synthase protein (43). Because no sequence homolog of *E. coli* CAT was identified in the *M. tuberculosis* genome, we investigated the possibility of 19cΔT interaction with PapA5. Our results showed that PapA5 formed a complex with 19cΔT although at much higher concentrations. Nonetheless, the 19cΔT-PapA5 interaction was highly specific as the FHA domain-containing protein GarA failed to form any physical contact with PapA5. Surprisingly, PapA5 displayed a fairly unusual interaction pattern with 19cΔT mutants. The mutation of Arg^{87} and Ser^{101}, shown to be detrimental for interaction of 19cΔT with PknB and CAT had a marginal impact on the 19cΔT-PapA5 interaction. Furthermore, the deletion of residues from 31 to 51 severely affected formation of the 19cΔT-PapA5 complex. A similar mutant, 19cFHA, formed a high affinity complex with PknB and CAT. We argued that the variable pattern of PapA5 interaction with 19cΔT mutants could possibly be due to the differential phosphorylation status of PapA5. Although PknB and CAT were purified as phosphorylated proteins, PapA5 was purified as an unphosphorylated protein from *E. coli*. Phosphoindependent interactions of the FHA domain-containing proteins have been previously reported for Chk2, the human homolog of *S. cerevisiae* Rad53 (30), and more recently for GarA (29). For Chk2, the phosphoindependent binding region located on the FHA domain was reported to be distinct from the conventional phosphopeptide binding motif, whereas for GarA the FHA surface forming contacts with the unphosphorylated proteins was shown to be similar to the Thr(P) binding surface. Furthermore, the minimal functional FHA domain of GarA-(55–149) was sufficient for its interaction with unphosphorylated target proteins and indeed caused more potent inhibition of target enzymes when compared with the full-length protein. However, the interaction studies on 19cΔT with PapA5 seem to suggest that 19cΔT forms phosphoindependent interactions primarily through the motif upstream of the functional FHA domain. The FHA domain plays a minimal role in phosphoindependent contacts of 19cΔT. As seen for the 19cΔT-PapA5 interaction, the phosphoindependent interaction of 19cΔT with PknBK40M, an autophosphorylation deficient mutant of PknB, was also found to depend on residues 31–51, further substantiating our hypothesis. Thus we propose that in the presence of phosphorylation on the target protein, 19cΔT interacts primarily through the critical residues in the FHA domain, whereas the upstream residues (residues 31–51) act cooperatively to stabilize the complex. In the absence of target protein phosphorylation the upstream residues primarily hold the complex because the interaction of these residues is expected to be independent of the phosphorylation status of the target protein.

Reversible Phosphorylation of PapA5 by the PknB-MstP Kinase Phosphatase Pair—The results discussed above clearly indicated that PapA5 could be a plausible target of PknB, and rightly so PapA5 was shown to be phosphorylated by PknB. PapA5 was modified exclusively on threonine residue(s) and phosphorylation was completely reversed by the serine/threonine phosphatase MstP. In the report on the crystal structure of PapA5, Buglino *et al.* (42) proposed that the interaction of PapA5 with its substrates through one of its solvent-exposed channels would require conformational changes. Phosphorylation could be one such modification bringing about the desired conformational changes. Alternatively PapA5 phosphorylation might affect its interaction with other components of PDIM biosynthesis (43) or with Rv0019c. In future, PapA5 phosphorylation and its interaction with Rv0019c if proven *in vivo* would provide a valuable link to regulation of the PDIM biosynthesis by PknB, thus providing another example of the profound effect of STPK-mediated phosphorylation in *M. tuberculosis* virulence.

REFERENCES

1. Wang, J. Y., and Koshland, D. E., Jr. (1978) *J. Biol. Chem.* **253,** 7605–7608
2. Muñoz-Dorado, J., Inouye, S., and Inouye, M. (1991) *Cell* **67,** 995–1006
3. Kennelly, P. J., and Potts, M. (1996) *J. Bacteriol.* **178,** 4759–4764
4. Av-Gay, Y., and Everett, M. (2000) *Trends Microbiol.* **8,** 238–244
5. Leonard, C. J., Aravind, L., and Koonin, E. V. (1998) *Genome Res.* **8,** 1038–1047
6. Yaffe, M. B., and Smerdon, S. J. (2004) *Annu. Rev. Biophys. Biomol. Struct.* **33,** 225–244
7. Koch, C. A., Anderson, D., Moran, M. F., Ellis, C., and Pawson, T. (1991) *Science* **252,** 668–674
8. Li, J., Lee, G. I., Van Doren, S. R., and Walker, J. C. (2000) *J. Cell Sci.* **113,** 4143–4249
9. Hofmann, K., and Bucher, P. (1995) *Trends Biochem. Sci.* **20,** 347–349
10. Liao, H., Byeon, I. J., and Tsai, M. D. (1999) *J. Mol. Biol.* **294,** 1041–1049
11. Hammet, A., Pike, B. L., Mitchelhill, K. I., Teh, T., Kobe, B., House, C. M., Kemp, B. E., and Heierhorst, J. (2000) *FEBS Lett.* **471,** 141–146
12. Li, J., Smith, G. P., and Walker, J. C. (1999) *Proc. Natl. Acad. Sci. U.S.A.* **96,** 7821–7826
13. Hammet, A., Pike, B. L., McNees, C. J., Conlan, L. A., Tenis, N., and Heierhorst, J. (2003) *IUBMB Life* **55,** 23–27
14. Durocher, D., Taylor, I. A., Sarbassova, D., Haire, L. F., Westcott, S. L., Jackson, S. P., Smerdon, S. J., and Yaffe, M. B. (2000) *Mol. Cell.* **6,** 1169–1182
15. Mahajan, A., Yuan, C., Lee, H., Chen, E. S., Wu, P. Y., and Tsai, M. D. (2008) *Sci. Signal.* **1,** re12
16. Pallen, M., Chaudhuri, R., and Khan, A. (2002) *Trends Microbiol.* **10,** 556–563
17. Hsu, F., Schwarz, S., and Mougous, J. D. (2009) *Mol. Microbiol.* **72,** 1111–1125
18. Mougous, J. D., Gifford, C. A., Ramsdell, T. L., and Mekalanos, J. J. (2007) *Nat. Cell Biol.* **9,** 797–803
19. Johnson, D. L., Stone, C. B., and Mahony, J. B. (2008) *J. Bacteriol.* **190,** 2972–2980
20. Johnson, D. L., and Mahony, J. B. (2007) *J. Bacteriol.* **189,** 7549–7555
21. Jelsbak, L., Givskov, M., and Kaiser, D. (2005) *Proc. Natl. Acad. Sci. U.S.A.* **102,** 3010–3015
22. Cole, S. T., Brosch, R., Parkhill, J., Garnier, T., Churcher, C., Harris, D., Gordon, S. V., Eiglmeier, K., Gas, S., Barry, C. E., 3rd, Tekaia, F., Badcock, K., Basham, D., Brown, D., Chillingworth, T., Connor, R., Davies, R., Devlin, K., Feltwell, T., Gentles, S., Hamlin, N., Holroyd, S., Hornsby, T., Jagels, K., Krogh, A., McLean, J., Moule, S., Murphy, L., Oliver, K., Osborne, J., Quail, M. A., Rajandream, M. A., Rogers, J., Rutter, S., Seeger, K., Skelton, J., Squares, R., Squares, S., Sulston, J. E., Taylor, K., Whitehead, S., and

Barrell, B. G. (1998) *Nature* **393,** 537–544
23. Wehenkel, A., Bellinzoni, M., Graña, M., Duran, R., Villarino, A., Fernandez, P., Andre-Leroux, G., England, P., Takiff, H., Cerveñansky, C., Cole, S. T., and Alzari, P. M. (2008) *Biochim. Biophys. Acta* **1784,** 193–202
24. Molle, V., Kremer, L., Girard-Blanc, C., Besra, G. S., Cozzone, A. J., and Prost, J. F. (2003) *Biochemistry* **42,** 15300–15309
25. Sharma, K., Gupta, M., Pathak, M., Gupta, N., Koul, A., Sarangi, S., Baweja, R., and Singh, Y. (2006) *J. Bacteriol.* **188,** 2936–2944
26. Papavinasasundaram, K. G., Chan, B., Chung, J. H., Colston, M. J., Davis, E. O., and Av-Gay, Y. (2005) *J. Bacteriol.* **187,** 5751–5760
27. Curry, J. M., Whalan, R., Hunt, D. M., Gohil, K., Strom, M., Rickman, L., Colston, M. J., Smerdon, S. J., and Buxton, R. S. (2005) *Infect. Immun.* **73,** 4471–4477
28. O'Hare, H. M., Durán, R., Cerveñansky, C., Bellinzoni, M., Wehenkel, A. M., Pritsch, O., Obal, G., Baumgartner, J., Vialaret, J., Johnsson, K., and Alzari, P. M. (2008) *Mol. Microbiol.* **70,** 1408–1423
29. Nott, T. J., Kelly, G., Stach, L., Li, J., Westcott, S., Patel, D., Hunt, D. M., Howell, S., Buxton, R. S., O'Hare, H. M., and Smerdon, S. J. (2009) *Sci. Signal*. **2,** ra12
30. Li, J., Williams, B. L., Haire, L. F., Goldberg, M., Wilker, E., Durocher, D., Yaffe, M. B., Jackson, S. P., and Smerdon, S. J. (2002) *Mol. Cell.* **9,** 1045–1054
31. Boitel, B., Ortiz-Lombardía, M., Durán, R., Pompeo, F., Cole, S. T., Cerveñansky, C., and Alzari, P. M. (2003) *Mol. Microbiol.* **49,** 1493–1508
32. Lu, Y. B., Ratnakar, P. V., Mohanty, B. K., and Bastia, D. (1996) *Proc. Natl. Acad. Sci. U.S.A.* **93,** 12902–12907
33. Boyle, W. J., van der Geer, P., and Hunter, T. (1991) *Methods Enzymol.* **201,** 110–149
34. Alderwick, L. J., Molle, V., Kremer, L., Cozzone, A. J., Dafforn, T. R., Besra, G. S., and Fütterer, K. (2006) *Proc. Natl. Acad. Sci. U.S.A.* **103,** 2558–2563
35. Molle, V., Soulat, D., Jault, J. M., Grangeasse, C., Cozzone, A. J., and Prost, J. F. (2004) *FEMS Microbiol. Lett.* **234,** 215–223
36. Grundner, C., Gay, L. M., and Alber, T. (2005) *Protein Sci.* **14,** 1918–1921
37. Young, T. A., Delagoutte, B., Endrizzi, J. A., Falick, A. M., and Alber, T. (2003) *Nat. Struct. Biol.* **10,** 168–174
38. Molle, V., Reynolds, R. C., Alderwick, L. J., Besra, G. S., Cozzone, A. J., Fütterer, K., and Kremer, L. (2008) *Biochem. J.* **410,** 309–317
39. Durán, R., Villarino, A., Bellinzoni, M., Wehenkel, A., Fernandez, P., Boitel, B., Cole, S. T., Alzari, P. M., and Cerveñansky, C. (2005) *Biochem. Biophys. Res. Commun.* **333,** 858–867
40. Villarino, A., Duran, R., Wehenkel, A., Fernandez, P., England, P., Brodin, P., Cole, S. T., Zimny-Arndt, U., Jungblut, P. R., Cerveñansky, C., and Alzari, P. M. (2005) *J. Mol. Biol.* **350,** 953–963
41. Leslie, A. G., Moody, P. C., and Shaw, W. V. (1988) *Proc. Natl. Acad. Sci. U.S.A.* **85,** 4133–4137
42. Buglino, J., Onwueme, K. C., Ferreras, J. A., Quadri, L. E., and Lima, C. D. (2004) *J. Biol. Chem.* **279,** 30634–30642
43. Trivedi, O. A., Arora, P., Vats, A., Ansari, M. Z., Tickoo, R., Sridharan, V., Mohanty, D., and Gokhale, R. S. (2005) *Mol. Cell.* **17,** 631–643
44. Onwueme, K. C., Ferreras, J. A., Buglino, J., Lima, C. D., and Quadri, L. E. (2004) *Proc. Natl. Acad. Sci. U.S.A.* **101,** 4608–4613
45. Durocher, D., and Jackson, S. P. (2002) *FEBS Lett.* **513,** 58–66
46. England, P., Wehenkel, A., Martins, S., Hoos, S., André-Leroux, G., Villarino, A., and Alzari, P. M. (2009) *FEBS Lett.* **583,** 301–307
47. Obsil, T., Ghirlando, R., Klein, D. C., Ganguly, S., and Dyda, F. (2001) *Cell* **105,** 257–267
48. Ganguly, S., Gastel, J. A., Weller, J. L., Schwartz, C., Jaffe, H., Namboodiri, M. A., Coon, S. L., Hickman, A. B., Rollag, M., Obsil, T., Beauverger, P., Ferry, G., Boutin, J. A., and Klein, D. C. (2001) *Proc. Natl. Acad. Sci. U.S.A.* **98,** 8083–8088
49. Li, H., Byeon, I. J., Ju, Y., and Tsai, M. D. (2004) *J. Mol. Biol.* **335,** 371–381